Laser-Induced Fluorescence of Base Adsorbed on Surface Sites in Solid Catalysts

**A. Lassoued,[1] J. Deson,[1] C. Lalo,[1] P. Batamack,[1] A. Gédéon,[1] and J. Fraissard[1,2]**

The interaction of quinoline with the surface of Nafion-H and Nafion-H (13 wt%)/silica gel composites, silica gel itself, HY zeolite, dealuminated or not, and two types of alumina is studied by laser-induced fluorescence. Strong Brønsted acid sites interact with quinoline to form the quinolinum, that ion being revealed by a band peaking at 390 nm. When Lewis acid sites are present, a complex formed between these sites and quinoline is observed. A dimeric species and the diffusion of the adsorbates on the surface of the Nafion-H polymer are discussed.

INTRODUCTION

Analysis of solid catalyst surfaces using laser-induced fluorescence (LIF) diagnosis [1] allows the characterization of species at a low density level. From the linear dependence of the intensity of the fluorescence upon the concentrations of the species on the solid surface, relative densities can be measured.

Under near-UV laser photoexcitation, quinoline (Q) adsorbed on the surface of thermally activated acidic solid catalysts (S—OH) has been shown to be a sensitive fluorescent probe for recognition of acidic surface sites [2,3]. Indeed, the protonation of this compound, which is well known to exhibit fluorescence only in polar media, leads to the formation of the quinolinium ion [Eq. (1)], and an increase in the fluorescence quantum yield is observed [4].

$$(1)$$
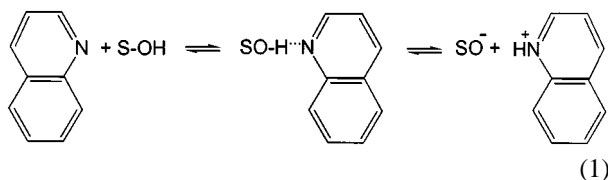
We report here on the measurement of the relative intensity of the quinolinium LIF band to compare the numbers of Brønsted acid sites of the surface of various solid catalysts, such as Nafion-H polymer alone and supported on silica, silica itself, acidic HY zeolites, dealuminated or not, and two types of alumina.

UV Spectroscopy of Quinoline

The energy levels [5] of the quinoline molecule correspond to the excitation of the π-bonding electrons of the ring and of the lone pair of nonbonding n electrons at nitrogen which are responsible for the basicity [6] of the compound. Quinoline is well known to exhibit only phosphorescence in nonpolar solvents when photoexcited in the near-UV [7,8]. This behavior can be explained by the presence of a triplet n,π^* state between the lowest singlet and triplet π,π^* states, enhancing intersystem

[1] Laboratoire de Chimie des Surfaces, UPMC-CNRS (ESA 7069), 4 place Jussieu, 75252 Paris Cedex 05, France.
[2] To whom correspondence should be addressed. Fax: 33.(0)1.4427.5536.

crossing (Scheme Ia). The structured fluorescence of quinoline, which is observed in polar solvents, is attributed to an inversion of the relative disposition of the triplet n,π^*-state and singlet π,π^*-state energy levels (Scheme Ib).

The complexation of quinoline in acidic polar solvents has been reported [7,8]. It has been shown [9] that with an increase in the strength of the field of an electron-acceptor species bonded to the quinoline molecule, there is a decrease in the spin-orbital interaction of the n electrons with the π electrons of the ring, which leads to an increase in the degree of conjugation of the π electrons and a lowering of energy levels with π,π^* character. Consequently, there is a slight displacement of the maximum of the radiation to longer wavelengths. Fluorescence spectra of charge-transfer complexes at 300 K are unstructured broad bands red-shifted compared to the fluorescence spectrum of quinoline. Like many large organic molecules, these species can be identified by two features of the fluorescence spectrum, the emission origin and the emission maximum.

In the present work, quinoline molecules are photoexcited at the edge of the third absorption band [10] at 240 nm (5.16 eV) well below the first ionization potential [4,8,11,12] at 8.6 eV. In this energy range there is vibronic coupling between states with π,π^* and n,π^* character, and photoexcitation can lead to an excited state with enhanced basicity, as reported for the first excited state [13,14].

Thus, the spectroscopic behavior of quinoline intercalated in the catalyst cavities must be influenced by the polarity of the medium and the presence of electron-acceptor or proton-donor sites.
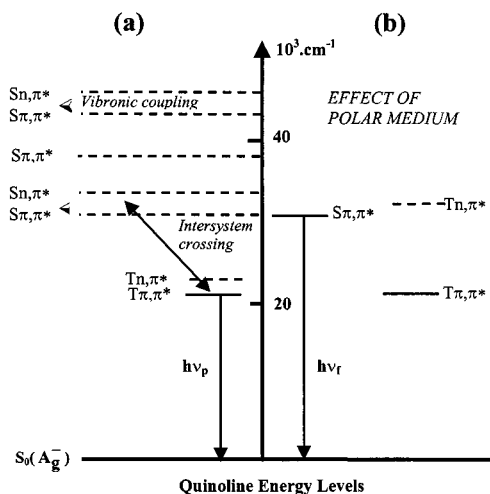
EXPERIMENTAL

Sample Characteristics

Three types of material from DuPont/Nemours (USA) were studied: silica gel,[3] Nafion-H, and Nafion-H (13 wt%)/silica gel composites. Their specific areas are 145, 0.1, and 200 m^2/g, respectively.

Nafion-H is a perfluorinated ion-exchange polymer which can be used as a hydrocarbon transformation catalyst. It has a homogeneous internal structure with a sequence of polar clusters of sulfonic acid groups that are dispersed with quasi-order throughout a hydrophobic, semicrystalline perfluorocarbon matrix [15]. In these clusters (3–5 nm), reactions are catalyzed by SO_3H groups. The superacidity [16,17] of the acid group is attributed to the electron-withdrawing ability of the perfluorocarbon backbone. However, the specific surface area of Nafion-H is low and molecules cannot diffuse easily to the acid sites. Nafion-H/silica gel with a higher surface area shows, in general, enhanced catalytic effects but the density of Nafion-H is lower. As a result, the characterization of acidic sites within Nafion-H/silica gel requires more sensitive detection methods.

Nafion-H (13 wt%)/silica gel was prepared using a slight modification of the literature method [18]. To 200 g of a 10 wt% solution of sodium silicate (10 wt% SiO_2 content) was added 100 g of a water-based 3 wt% Nafion-containing solution. HCl (ca. 52 g of a 3.5 M solution) was added to adjust the pH to about 7. The system gels, and the gel is dried in flowing nitrogen at 368–373 K. The hard, dried gel is thoroughly washed with 25 wt% nitric acid and, finally, vacuum-dried. The number of acid equivalents was determined to be about 0.15 mEq per g. For comparison, amorphous samples of a Davidson silica were investigated.

HY zeolite was UOP NH_4Y zeolite, denoted Y64. D-HY zeolite was prepared from NH_4Y. It was partially dealuminated by steaming and subsequently washed twice with Na_2H_2EDTA; its crystallinity is near 90%. Previous studies [19] using ^{27}Al-NMR have shown that these two samples contain no extraframework aluminum. ^{29}Si-NMR results indicate that Si/Al = 2.4 for HY and 14.5 for D-HY. The number of Na per unit cell is given

Scheme I. (a) Energies of low-lying states of quinoline. (b) Effect of polar medium. State energies which were determined experimentally [7,10] are indicated by solid lines; dashed lines denote calculated values [5].

by chemical analysis. This result indicates that the number of Brønsted acid sites per unit cell is 47.7 and 14.5 for HY and D-HY, respectively. For the dealuminated specimen, the Lewis acid-to-Brønsted acid site ratio is 0.12 ± 0.02, given by ^{1}H-NMR at 4 K performed on the D-HY after adsorption of a known amount of H_2O [20].

Two types of industrial alumina with different preparation processes were examined also. Their characterization by ^{1}H-NMR does not give any information concerning their acidity [21].

All samples were activated under "shallow-bed conditions": a powder layer less than 10 mm thick and dehydration under dynamic vacuum before and during heating at 12 K h^{-1} to 450 K for Nafion-H and Nafion-H/silica gel and to 600 K for the silica and alumina samples, the maximum temperature being maintained for 16 h before cooling to room temperature.

Quinoline vapor was adsorbed at 300 K. The amount of quinoline in each sample was determined volumetrically and gravimetrically. The samples prepared contain 0.3 ± 0.1 mg of quinoline per g of adsorbent ($\approx 2.3 \cdot 10^{-3}$ mol/g).

Experimental Technique

In a quartz optical cell under vacuum (10^{-4} Pa), the samples were photoexcited using a frequency-doubled dye laser, and the fluorescence was recorded from 300 to 600 nm. The apparatus was described previously [1]. The laser emitted at 240 nm, the pulse width being about 30 ns. The size of the beam was adjusted by a dispersing lens and a diaphragm so as to obtain maximum coverage of the sample. Luminescence was detected perpendicularly to the laser beam through a quartz collecting lens by a photomultiplier (Hamamatsu R212UH) at the exit slit of a monochromator and stored in a gated integrator. Signal decay at selected wavelengths was recorded with a digital storage oscilloscope (Tektronics 2432) and transferred to a microcomputer (PC compatible), the limit of the detection system being 1 μs. Computer processing of the measurements consisted of a deconvolution of the multiexponential signal decay. For luminescence with lifetimes of less than 1 μs, the decomposition of the spectra into Gaussian bands is based on the literature data [4,22]. Table I lists the features of well-known emitting centers, quinoline itself, quinoline dimer, the H-bonded quinoline complex, and the quinolinium ion.

Quantitative LIF Spectroscopy

The function allowing quantitative determination of the species concentration C from the total laser-induced

Table I. Fluorescence Band Characteristics

Species	Origin (nm)	Maximum (nm)	Ref. No. (s.)
Quinoline Q	300	330	4, 22
Quinoline dimer	350	440	22
H-bonded complex, Q···H	320	370	4
Quinolinium ion, [+]QH	350	390	4

fluorescence (LIF) signal S_{LIF} in the case of a two-level system can be written

$$S_{LIF} = (E(\nu)/h\nu)(\sigma C)\Phi \qquad (2)$$

where $E(\nu)$ is the laser energy per pulse at frequency ν, $h\nu$ the energy of the absorption transition from the ground to the excited singlet states of the species to be examined, σ the absorption cross section which is related to the oscillator strength of the transition, C the species concentration, and Φ the fluorescence yield, which depends on the collisional quenching rate of the upper singlet state. The terms in parentheses in the equation correspond to the number of photons at frequency ν incident on the observation volume and to the fraction of photons absorbed, respectively; Φ corresponds to the fraction of photons reemitted [23].
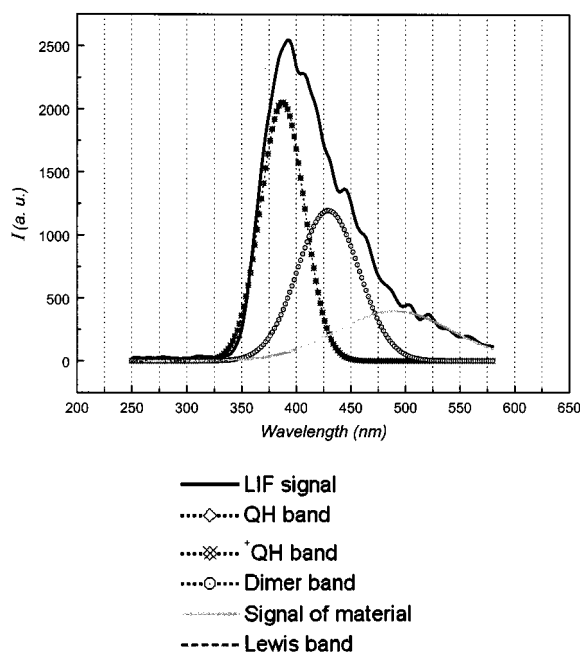

Fig. 1. Decomposition of the LIF spectrum of quinoline adsorbed on Nafion-H (0.2 mg quinoline/g adsorbent). Note that the key in Fig. 1 applies to all figures in this paper.

According to Eq. (2), the total signal intensity is expected to depend linearly on the species concentration as well as on the intensity of the UV radiation. Consequently, to obtain a quantitative estimate of the relative concentrations of the species in the various samples, it is important, first, to check that the laser-induced luminescence signal intensity is linearly dependent on the laser intensity and, then, to perform the measurements under the same conditions.

Lifetime Measurements

The intensity of a luminescence from an excited state decays exponentially with the time after the laser pulse:

$$I = I_0 \exp(-t/\tau) \qquad (3)$$

The mean lifetime τ, which is a characteristic of this excited state, is related to the rates of all its deactivation processes. Without collision phenomena, it is expressed by

$$\tau = 1/(k_r + k_{ic}) \qquad (4)$$

where k_r refers to the rate constant for emission and k_{ic} to the rate constant for internal conversion by vibrational relaxation, which depends on the environment.

In the case of alumina samples, photoexcitation of the material leads to a phosphorescence, and, from the multiexponential decay of this luminescence, the contribution of independent emitting centers can be determined [2].

SPECTRUM OF QUINOLINE ADSORBED ON THE CATALYST SURFACE

Nafion-H

Decomposition of the LIF Spectrum

In Nafion-H, quinoline interacts with proton-donor sulfonic acid groups in polar clusters accessible to quinoline molecules [3]. UV photoexcitation of quinoline adsorbed on a Nafion-H surface leads to a very intense short-lived LIF signal. The LIF spectrum is processed using Gaussian decomposition based on data listed in Table I. As shown in Fig. 1, the decomposition of the luminescence spectrum reveals that, in addition to a weak luminescence of the material at 500 nm detected without quinoline, two bands are observed. The strongest, peaking at 390 nm with an emission origin at 350 nm, corresponds to the fluorescence of the quinolinium ion which is formed when quinoline interacts with Brønsted sites. A second band, with its origin at 350 nm and maximum at 430 nm,
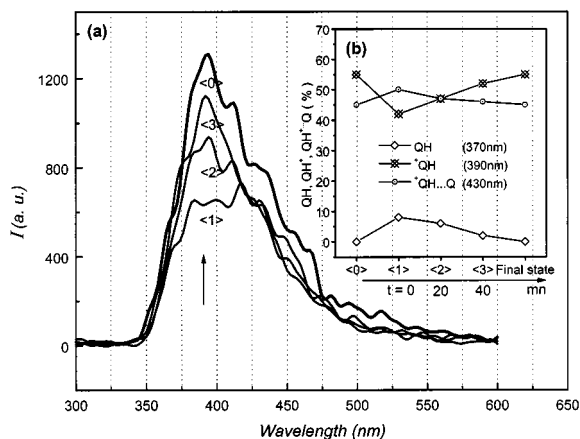

Fig. 2. Diffusion of adsorbates on the Nafion-H surface. (a) LIF spectra. (b) Decomposition of the LIF spectra: time dependence of the LIF signal for the H-bonded complex, quinolinium ion, and dimeric species.
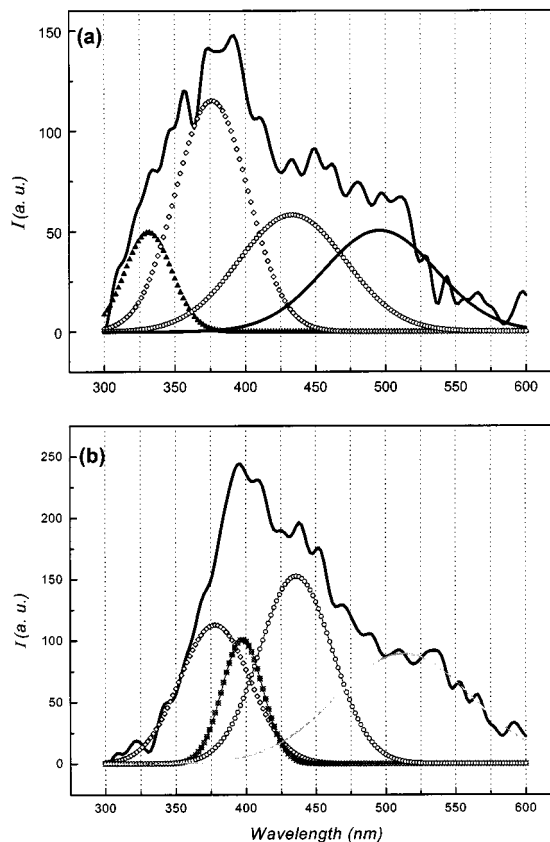

Fig. 3. Decomposition of the LIF spectrum of quinoline adsorbed on silica (0.2 mg quinoline/g adsorbent). (a) DuPont silica. (b) Davidson silica.

corresponds to a dimeric species. We tentatively attribute this second component to the fluorescence of a dimeric $^+$QH$\cdots$Q species characterized by a strong $^+$NH$\cdots$N hydrogen bond, which could be formed by interaction between the quinoline and the quinolinium ion. This type of dimeric species has been identified in the case of the interaction of pyridine with Nafion-H [24].

$$^+QH + Q \Leftrightarrow {}^+QH\cdots Q \qquad (5)$$
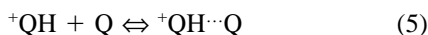
Diffusion of Adsorbates on the Nafion-H Surface

Diffusion of adsorbates on the Nafion-H surface was studied. The first LIF spectrum, denoted spectrum ⟨0⟩, was recorded 12 h after adsorbing 0.2 mg/g of quinoline. The spectrum obtained is unchanged over 10 days (Fig. 2a; ⟨0⟩). Spectrum ⟨1⟩ corresponds to the first recording directly after the addition of 0.2 mg quinoline/g adsorbent to the above sample. Spectra ⟨2⟩ and ⟨3⟩ were recorded 20 and 40 min, respectively, after spectrum ⟨1⟩. The fluorescence band intensity characteristic of the quinolinium ion seems to increase with time; the shape of the spectrum also tends to that of spectrum ⟨0⟩.

Decomposition of the spectra reveals three bands corresponding to the H-bonded complex Q$\cdots$H, the quinolinium ion $^+$QH, and the dimeric species $^+$QH$\cdots$Q. Figure 2b reports the time dependence of the LIF signal characteristic of these species: the intensity of the H-bonded complex band decreases with time and disappears, while, conversely, the quinolinium LIF band intensity increases. This phenomenon could be related to the mobility of excited single-bonded adsorbates with low binding energies, which favor translational motion; their dissociation could be followed by the diffusion of quinoline on Brønsted sites [25].
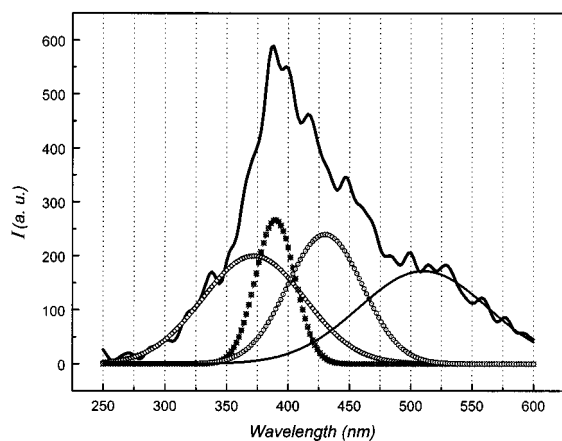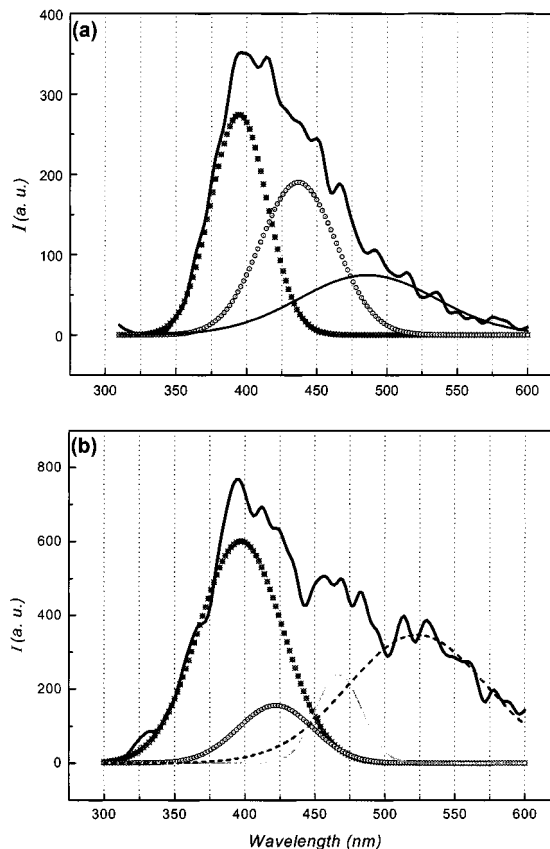

Fig. 5. Decomposition of the LIF spectrum of quinoline adsorbed on zeolites (0.2 mg quinoline/g adsorbent). (a) HY zeolite. (b) Dealuminated HY zeolite.

The relative intensities of the $^+$QH and dimeric species bands increase to a constant ratio. This ratio does not change over a period of 10 days. Spectrum ⟨3⟩ progresses to the same shape as ⟨0⟩. It seems that this ratio is related to the distribution of acidic sites on the surface.

Silica

For amorphous silica gel samples dehydrated at 600 K, the luminescence induced by photoexcitation is weak and decomposition of the LIF spectra observed for two types of silica, DuPont and Davidson, reveals different Brønsted acid strengths. The Gaussian decomposition based on data given in Table I is illustrated in Figs. 3a and b.

For DuPont silica gel (Fig. 3a), three major bands, peaking at 325, 370, and 440 nm, can be readily assigned: the first one, with an emission origin at 300 nm, corresponds to the fluorescence of quinoline and the third one to the fluorescence of the quinoline dimer, while the second band corresponds to the fluorescence of a hydro-
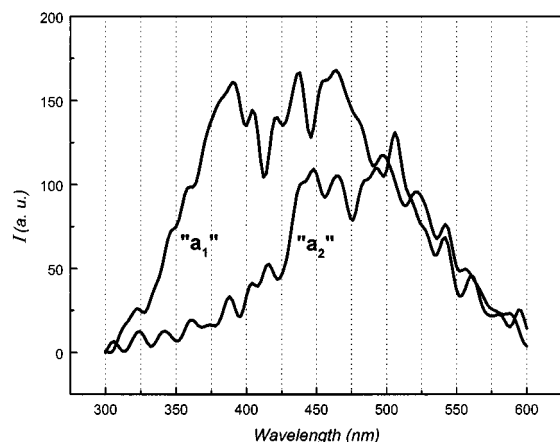

Fig. 4. Decomposition of the LIF spectrum of quinoline adsorbed on Nafion-H/silica gel composites (0.2 mg quinoline/g adsorbent).

Fig. 6. LIF spectrum of quinoline adsorbed on two types of alumina, a₁ and a₂ (0.2 mg quinoline/g adsorbent).

gen-bonded complex. As reported by Eremenko *et al.* [14], UV irradiation seems to favor the adsorption of quinoline which forms H-bonded complexes with silanol groups. The fourth band, peaking at 490 nm, is that of the material.

For Davidson silica (Fig. 3b), decomposition of the LIF spectrum reveals three bands, peaking at 370, 390, and 430 nm, which have the features of the fluorescence of the H-bonded complex, the ion quinolinium $^+$QH, and the dimeric species $^+$QH$\cdots$Q, respectively. It then appears that, in contrast to DuPont silica gel, where adsorption sites seem to be nonacidic, in Davidson silica proton-donor sites are present. Magic angle spinning (MAS) and broad-line ^{1}H-NMR at a low temperature (4 K) would provide additional information about the acidity of these samples.

Nafion-H/Silica Gel DuPont Composites

In Nafion-H/silica gel composites with a high specific area, the adsorption sites are sulfonic acid groups within the Nafion-H phase and nonacid silanol groups within the silica gel phase [3]. In this case, we observe that the luminescence intensity is significantly lower than for Nafion-H samples and higher than for the DuPont silica sample. Decomposition of the spectrum (Fig. 4) reveals the same components peaking at 390 and 430 nm already observed with Nafion-H. These bands are characteristic of the fluorescence of quinolinium ion and of the dimeric species $^+$QH$\cdots$Q. In addition, the fluorescence of the H-bonded complex peaking at 370 nm is observed. This is characteristic of the interaction of quinoline with silanol groups in the silica gel phase, which
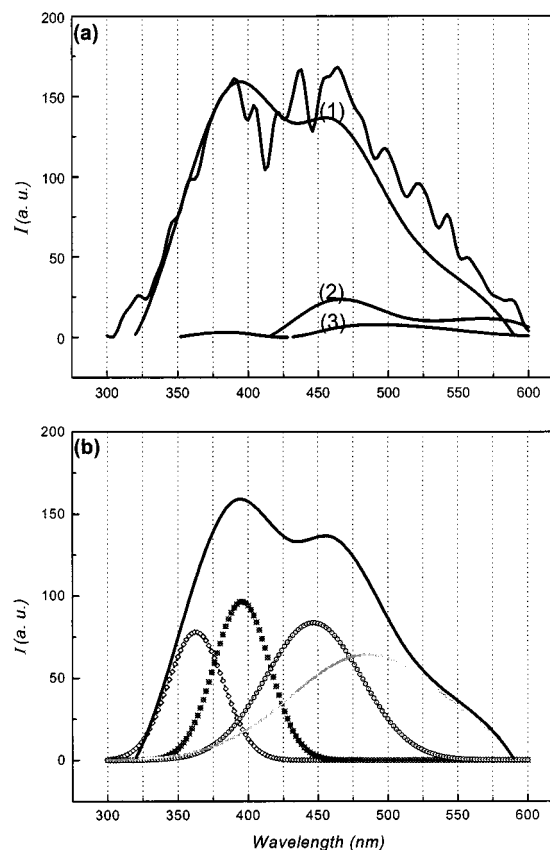

Fig. 7. (a) Time-resolved decomposition of the laser-induced luminescence for alumina a₁ (0.2 mg quinoline/g adsorbent): (1) short-lived component, (2) medium-lived component, and (3) long-lived component. (b) Spectral deconvolution of the short-lived component.

implies that the silica surface is not totally covered with Nafion-H.

Acidic Y Zeolites

Y zeolites are organized media which have a homogeneous internal structure with a well-defined sequence of cages. Their efficiency as heavy oil-cracking catalysts depends on the acidic surface sites accessible to the hydrocarbon molecules. These sites located in the supercages are primary adsorption centers for basic compounds. In HY zeolites, whether dealuminated or not, the protonation of quinoline on Brønsted sites is characterized by the fluorescence of the quinolinium ion peaking at 390 nm together with the fluorescence of the dimeric species $^+$QH$\cdots$Q peaking at 430 nm (Fig. 5a). In dealuminated HY, a complexation of quinoline with electron-acceptor Lewis sites is characterized by an additional band at 520 nm, the fluorescence of a charge-transfer complex being strongly red-shifted (Fig. 5b).

Alumina

Two types of alumina, denoted a_1 and a_2, were studied. They exhibit an intrinsic luminescence under photoexcitation. When quinoline was adsorbed on the surface, while no change in the luminescence spectrum was observed for specimen a_2, that of a_1 seems to be more extended on the blue side (Fig. 6).

From a kinetic study of the decay of the photoinduced luminescence in alumina a_1, the contribution of three components with specific lifetimes of 100, 20, and <1 μs can be observed. The most intense short-lived band involves adsorbed quinoline (Fig. 7a). Decomposition of this band shows three bands, peaking at 370, 390, and 430 nm, which can be readily assigned to the fluorescence of the H-bonded complex, the quinolinium ion, and a dimeric quinoline species, respectively (Fig. 7b). It then appears that, in contrast to alumina a_2, proton-donor sites are detectable in alumina a_1.

QUANTITATIVE RESULTS

Under the same conditions of laser intensity, we measured the relative intensity of the quinolinium ion band in the various solid catalyst samples with 0.2 mg quinoline/g adsorbent (Fig. 8). The quinolinium LIF band seems to be the most intense for Nafion-H specimens, showing that the density of $^+$QH is highest on the Nafion-H surface. The density of $^+$QH seems to be one order of magnitude lower for HY and dealuminated HY (D-HY) zeolites and more than one order of magnitude weaker in the case of Nafion-H/silica gel nanocomposites.
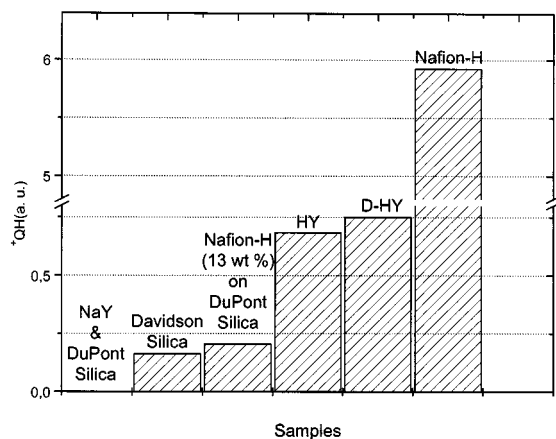

Fig. 8. LIF signal intensity of quinolinium ion for various catalyst surfaces with adsorbed quinoline (0.2 mg quinoline/g adsorbent).

A similar density of $^+$QH is obtained for HY and D-HY zeolites. Much $^+$QH$\cdots$Q is observed with HY; this is due to the fact that in D-HY, quinoline is first adsorbed on Lewis sites, at the expense of the formation of dimeric species.

CONCLUSION

This study leads to a first estimate of the relative numbers of Brønsted acid sites of various solid catalyst surfaces using the LIF technique. However, to estimate the total numbers of acidic sites of the various catalysts, the concentration of the dimeric species $^+$QH$\cdots$Q must be taken into account as well as that of the quinolinium ion $^+$QH. The concentrations of these two species on the surface are related to the environment of the acidic sites and to the amount of quinoline adsorbed. The fraction of the dimeric species gives an idea of the distribution of acidic sites on the surface. When Brønsted sites are very close, the formation of the dimeric species is more probable.

REFERENCES

1. J. Deson, C. Lalo, A. Gédéon, F. Vasseur, and J. Fraissard (1996) *Chem. Phys. Lett.* **258**, 381.
2. C. Lalo, J. Deson, A. Gédéon, and J. Fraissard (1997) *Chem. Phys. Lett.* **279**, 230.
3. A. Lassoued, C. Lalo, J. Deson, P. Batamack, J. Fraissard, M. A. Hamer, and D. Corbin (1999) *Chem. Phys. Lett.* **303**, 368.
4. W. R. Moomaw and M. F. Anton (1976) *J. Phys. Chem.* **80**, 2243.
5. J. D. Baber and M. C. Zerner (1991) *J. Phys. Chem.* **95**, 8614.
6. I. Y. Martynov, A. B. Demyashkevich, B. M. Uzhinov, and M. G. Kuz'min (1977) *Russ. Chem. Rev.* **46**, 1.
7. R. Snyder and A. C. Testa (1984) *J. Phys. Chem.* **88**, 5948.
8. W. R. Moomaw, D. A. Kleier, J. H. Markgraf, J. W. Thoman, J. Neil, and A. Ridyard (1988) *J. Phys. Chem.* **92**, 4892.
9. A. V. Karyakin, T. S. Sorokina, and M. G. Skvortsov (1982) *Opt. Spectrosc.* **52**, 26.
10. H. Baba and I. Yamazaki (1972) *J. Mol. Spectrosc.* **44**, 118.
11. M. F. Anton and W. R. Moomaw (1977) *J. Chem. Phys.* **66**, 1808.
12. M. F. Anton and M. Nicol (1979) *J. Luminesc.* **18/19**, 131.
13. S. A. Samchuk, O. I. Kozik, N. P. Smirnova, A. M. Eremenko, V. A. Pokrovskii, and A. A. Chuiko (1991) *Russ. J. Phys. Chem.* **65**, 386.
14. A. M. Eremenko, N. P. Smirnova, S. A. Samchuk, and A. A. Chuiko (1992) *Coll. Surf.* **63**, 83.
15. Q. Deng, Y. B. Moore, C. L. McCormick, and K. A. Mauritz (1997) *Chem. Mater.* **9**, 36.
16. G. A. Olah, G. K. S. Prakash, and J. Sommer (1985) *Superacids*, Wiley Interscience, New York.
17. J. Grondin, R. Sagnes, and A. Commeyras (1976) *Bull. Soc. Chim. Fr.* **1**, 779.
18. (a) M. A. Harmer, W. E. Farneth, and Q. Sun (1996) *J. Am. Chem. Soc.* **118**, 7708. (b) A. Lassoued, C. Lalo, J. Deson, P. Batamack J. Fraissard, M. A. Harmer, and D. Corbin (1999) *Chem. Phys. Lett.* **303**, 368.

19. L. Heeribout, V. Semmer, P. Batamack, C. Dorémieux-Morin, R. Vincent, and J. Fraissard (1996) in J. W. Hightower, W. N. Deglass, E. Iglesia, and A. T. Bell (Eds.), *Studies in Surface Science and Catalysis (B)*, 11th International Congress on Catalysis, Elsevier, Amsterdam, pp. 831–840.
20. L. Heeribout, V. Semmer, P. Batamack, C. Dorémieux-Morin, and J. Fraissard (1995) *J. Chem. Soc. Faraday Trans.* **91**, 23.
21. A. Lassoued, C. Lalo, J. Deson, P. Batamack, and J. Fraissard, unpublished results.

22. R. P. Blaustein and K. S. Gant (1973) *Photochem. Photobiol.* **18**, 347.
23. M. P. Lee and R. K. Hanson (1986) *J. Quant. Spectrosc. Radiat. Transfer* **365**, 425.
24. R. Buzzoni, S. Bordiga, G. Ricchiardi, C. Lamberti, A. Zecchina, and G. Bellusi (1996) *Langmuir* **12**, 930.
25. D. Oelkrug, W. Flemming, R. Fullemann, R. Günther, W. Honnen, G. Krabichler, M. Schäfer, and S. Uhl (1986) *Pure Appl. Chem.* **58**, 1207.